Neuroradiology (2021) 63:217–224
https://doi.org/10.1007/s00234-020-02528-3

FUNCTIONAL NEURORADIOLOGY

Corticospinal tract involvement in spinocerebellar ataxia type 3: a diffusion tensor imaging study

Bruno Shigueo Yonekura Inada[1,2] · Thiago Junqueira Ribeiro Rezende[3] · Fernando Vieira Pereira[1] · Lucas Ávila Lessa Garcia[4] · Antônio José da Rocha[5] · Pedro Braga Neto[6,7] · Orlando Graziani Povoas Barsottini[1] · Marcondes Cavalcante França Jr[3] · José Luiz Pedroso[1]

Received: 18 June 2020 / Accepted: 16 August 2020 / Published online: 2 September 2020

Abstract

Purpose The aim of this study was to evaluate the integrity of the corticospinal tracts (CST) in patients with SCA3 and age- and gender-matched healthy control subjects using diffusion tensor imaging (DTI). We also looked at the clinical correlates of such diffusivity abnormalities.

Methods We assessed 2 cohorts from different Brazilian centers: cohort 1 ($n = 29$) scanned in a 1.5 T magnet and cohort 2 ($n = 91$) scanned in a 3.0 T magnet. We used Pearson's coefficients to assess the correlation of CST DTI parameters and ataxia severity (expressed by SARA scores).

Results Two different results were obtained. Cohort 1 showed no significant between-group differences in DTI parameters. Cohort 2 showed significant between-group differences in the FA values in the bilateral precentral gyri ($p < 0.001$), bilateral superior corona radiata ($p < 0.001$), bilateral posterior limb of the internal capsule ($p < 0.001$), bilateral cerebral peduncle ($p < 0.001$), and bilateral basis pontis ($p < 0.001$). There was moderate correlation between CST diffusivity parameters and SARA scores in cohort 2 (Pearson correlation coefficient: 0.40–0.59).

Conclusion DTI particularly at 3 T is able to uncover and quantify CST damage in SCA3. Moreover, CST microstructural damage may contribute with ataxia severity in the disease.

Keywords Spinocerebellar ataxia type 3 · Machado-Joseph disease · Cerebellar ataxia · Corticospinal tract · Diffusion tensor imaging · Retrograde degeneration

Introduction

Spinocerebellar ataxia type 3 (SCA3) or Machado-Joseph disease (MJD) is the most common autosomal dominant spinocerebellar ataxia (SCA) worldwide and is caused by a CAG trinucleotide expansion located in exon 10 of *ATXN3* [1]. This is a neurodegenerative disorder that typically begins in the 3rd or 4th decade of life. The clinical spectrum of SCA3 includes variable degrees of cerebellar ataxia, ophthalmoplegia, nystagmus, pyramidal and extra-pyramidal signs, and also non-motor symptoms [2–5]. Several clinical, imaging, and pathological studies in SCA3 have demonstrated widespread neurodegeneration, with involvement of the brainstem, basal ganglia, spinal cord, peripheral nerves,

✉ Bruno Shigueo Yonekura Inada
brunosy.inada@gmail.com

[1] Division of General Neurology and Ataxia Unit, Department of Neurology, Federal University of São Paulo (UNIFESP), São Paulo, Brazil

[2] Department of Neuroradiology, Hospital Beneficência Portuguesa, São Paulo, Brazil

[3] Department of Neurology, State University of Campinas (UNICAMP), São Paulo, Brazil

[4] Department of Neuroradiology, University of São Paulo (USP), São Paulo, Brazil

[5] Department of Neuroradiology, Santa Casa de São Paulo School of Medical Sciences, São Paulo, Brazil

[6] Department of Clinical Medicine, Universidade Federal do Ceará, Ceará, Brazil

[7] Center of Health Sciences, Universidade Estadual do Ceará, Ceará, Brazil

cerebral cortex, and the cerebellum [6–9]. Pyramidal signs such as brisk tendon reflexes and spasticity are common, and reflect involvement and degeneration of the corticospinal tracts (CST).

Neuroimaging studies have proven useful to characterize the extension of CNS damage and to track progression of SCA3. MRI-derived parameters may turn into potential biomarkers to assist in the design of clinical trials for SCA3. However, these studies mostly focused in the cerebellum and connections [9–11]. Few articles have evaluated the CST in SCA3. Neurophysiological studies with transcranial magnetic stimulation demonstrated alteration in cortical excitability and central motor conduction time, suggesting motor system neurodegeneration [12, 13]. Other DTI studies showed widespread white matter damage in SCA3 patients, including in the CST [14, 15]. In this scenario, diffusion tensor imaging (DTI) emerges as an interesting tool to investigate damage to this tract. It is an MRI technique that uses different gradient directions to generate images based on the random motion of water molecules. DTI provides quantitative measures of magnitude and direction of water molecules, using different measures, like fractional anisotropy (FA), mean diffusivity (MD), radial diffusivity (RD) and axial diffusivity (AD). These metrics are considered surrogate markers of the microstructural integrity of white matter tracts in the brain.

Therefore, considering that pyramidal signs are frequent in SCA3, the aim of this study is to characterize the pattern of CST damage in the disease using DTI. We also looked at the clinical correlates of such diffusivity abnormalities.

Materials and methods

Subject's selection

We retrospectively evaluated 120 patients with clinical and genetically confirmed SCA3 from Ataxia Outpatient Clinic at UNIFESP hospital and from Neurogenetics Outpatient Clinic at UNICAMP hospital. We divided those subjects in 2 cohorts: cohort 1 included 29 patients from the UNIFESP Ataxia Outpatient Clinic that were scanned in a 1.5 T MRI; cohort 2 included 91 patients from the UNICAMP Neurogenetics Outpatient Clinic that underwent 3.0 T MRI.

A control group of 120 age- and gender-matched healthy individuals underwent MRI scans and results were compared with SCA3 patients. Twenty-nine control subjects were from UNIFESP and were scanned in a 1.5 T MRI. Ninety-one control subjects were from UNICAMP and were scanned in a 3.0 T MRI.

Institutional ethics committee (Comitê de ética em Pesquisa da UNIFESP) approved this study and written informed consent was obtained from all participants.

Clinical evaluation

All SCA3 patients were evaluated with neurological examination and the Scale for the Assessment and Rating of Ataxia (SARA) [16]. The interval between clinical evaluation and MRI scanning was no more than 1 month. Some demographical and clinical features such as age at onset, disease duration, and CAG repeat length were also collected.

Imaging acquisitions

Cohort 1 Twenty-nine SCA3 patients and twenty-nine control subjects underwent a high-resolution MRI acquisition on a 1.5 T Phillips Achieva Scanner. Imaging acquisition was made using a standard 8-channel head coil. For DTI multi-atlas analyses, we used a single shot echo planar DTI sequence: $2.2 \times 2.2 \times 2.2$ mm^3 acquiring voxel size, interpolated to $1 \times 1 \times 1$ mm^3; reconstructed matrix of 128×128; TE/TR 70/8156 ms; flip angle 90°; 32 gradient directions; no averages; max *b*-factor = 700 s/mm^2. For T1 multi-atlas, we used high-resolution T1 volumetric images of the brain with axial orientation, voxel matrix 256×256, voxel size $1 \times 1 \times 1.1$ mm^3, TR/RE 7.7/3.8 ms, and flip angle 8°.

Cohort 2 Ninety-one SCA3 patients and ninety-one control subjects underwent a high-resolution MRI acquisition on a 3.0 T Phillips Achieva Scanner. Imaging acquisition was made using a standard 8-channel head coil. For DTI multi-atlas analyses, we used a spin echo DTI sequence: $2 \times 2 \times 2$ mm acquiring voxel size, interpolated to $1 \times 1 \times 2$ mm^3; reconstructed matrix 256×256; TE/TR 61/8500 ms; flip angle 90°; 32 gradient directions; no averages; max *b*-factor = 1000 s/mm^2. For T1 multi-atlas, we used a high-resolution T1 volumetric images of the brain with sagittal orientation, voxel matrix $240 \times 240 \times 180$, voxel size $1 \times 1 \times 1$mm^3, TR/TE 7/3.201 ms, and flip angle 8°.

A routine T2-weighted sequence and fluid-attenuated inversion recovery (FLAIR) was performed in all subjects and carefully reviewed by a board-certified neuroradiologist (Inada BSY) in order to rule out unrelated abnormalities. No patients were excluded due to poor image quality.

DTI analysis

To process the DTI images, we used a web-based service for multi-contrast imaging segmentations and quantification—"MRICloud" (MRICloud.org). To remove subject motion, the raw DTI images were corrected for eddy currents and co-registered [17] using a 12-pareameter affine transform [18]. We used a multivariate linear fitting to quantify the DTI parameters. To skull-strip, we used the intensity threshold using a $b = 0$ image with a tool of RoiEditor software (Li, X.; Jiang, H.; Yue, Li.; and Mori, S.; Johns Hopkins University,

www.MriStudio.org or www.kennedykrieger.org). After that, we employed the multi-contrast LDDMM algorithm to register the atlas to the images and then the parcellation, which employs a DLFA algorithm [19]. All analyses are performed in native space. The computations were processed on the Gordon cluster of XSEDE [20].

DTI multi-atlas automatically segmented the brain white matter in 59 labels. We choose the following segments to study the CST: precentral gyrus (PCG), superior corona radiata (SCR), posterior limb of internal capsule (PLIC), cerebral peduncle (CP), and basis pontis (BP) (Fig. 1). Afterwards, we computed the values of FA, MD, RD, and AD separately for all previously mentioned labels.

Statistical analysis

We used descriptive statistics to report the major findings. Age variance and distribution were accessed with Levene's test and skewness normality test. For each variable of interest, the Shapiro-Wilk test was employed to assess the presence of a normal distribution. The inferential analysis utilized the one sample *t* test (intragroup differences) or the two samples *t* test (intergroup differences).

Correlation degree and the level of interaction between quantitative variables were verified by utilizing Pearson correlation coefficient (PCC). The strength of PCC was described by using the following guide: very weak: 0.00–0.19; weak: 0.20–0.39; moderate: 0.40–0.59; strong: 0.60–0.79; very strong: 0.80–1.00.

For all comparisons, the level of significance was set at 0.05, corrected for multiple comparisons with post hoc Tukey_HSD test. We used the software SPSS (version 25) to run the analyses.

Results

Cohort 1

No differences were observed between SCA3 subjects and the respective control group regarding age (40.5 ± 10.5 vs 42.5 ± 9.6 years, $p = 0.4$) and gender (16 females and 13 males in SCA3 subjects and control). The mean disease duration was 7.1 ± 4.2 years (ranging from 2 to 20 years). The mean CAG repeat length was 71.0 ± 3.7 (ranging from 63 to 77). Mean SARA score was 10.8 ± 6.6 (ranging from 1 to 25.5).

DTI analysis showed reduction in FA values in bilateral PCG in SCA3 subjects (right side: 0.572 ± 0.037 vs 0.593 ± 0.016, $p = 0.007$; left side: 0.591 ± 0.036 vs 0.610 ± 0.011, $p = 0.009$.).

We did not find reduction in FA values in the SCR, PLIC, CP, and BP. We did not find either significant differences in MD, RD, and AD values comparing patients and controls (Table 1).

There was no significant correlation between disease duration, SARA, and CAG repeat length and any of the DTI-derived parameters.

Cohort 2

No differences were observed between SCA3 subjects and the respective control group regarding age (48.16 ± 12.79 vs 47.92 ± 12.5, $p = 0.8$) and gender (49 females and 42 males in SCA3 subjects and control). The mean disease duration was 10.38 ± 6.82 years (ranging from 0 to 34 years). The mean CAG expansion length in SCA3 patients was 71.93 ± 3.69 (ranging from 64 to 83). Mean SARA score in SCA3 patients was 13.13 ± 8.63 (ranging from 0 to 31).

FA: The SCA3 group showed decrease in FA in bilateral PCG, SCR, PLIC, CP, and BP (Table 2).

MD: The SCA3 group showed increased MD in left PCG, bilateral SCR, bilateral PLIC, bilateral CP, and bilateral BP (Table 2). We did not find significant reduction in MD values in right PCG in SCA3 subjects.

RD: The SCA3 group showed increased RD in bilateral PCG, SCR, PLIC, CP, and BP (Table 2).

AD: The SCA3 group showed increased AD in bilateral PLIC, bilateral BP, and left CP compared with the respective control group. We did not find significant increase at the PCG, bilateral SCR, and right CP (Table 2).

In order to find the most affected segment of the CST, we calculated the mean value difference (in percentage) of FA, MD, RD and AD between the SCA3 subjects of the cohort 2 and the respective control group in all segments of this tract (Fig. 2).

Correlation analyses PCG, SCR, PLIC, CP, and BP demonstrate moderate negative correlation between FA values and SARA scores, and moderate positive correlation of MD and RD values with SARA scores. We also identified a weak positive correlation between SARA scores and AD values for these regions. Furthermore, there was no significant correlation between disease duration or CAG repeat length and any of the DTI-derived parameters (Online resource).

Discussion

In this study, DTI was employed to evaluate the CST in SCA3 patients from 2 different institutions. We looked at 4 DTI parameters: FA and MD are the most popular measures

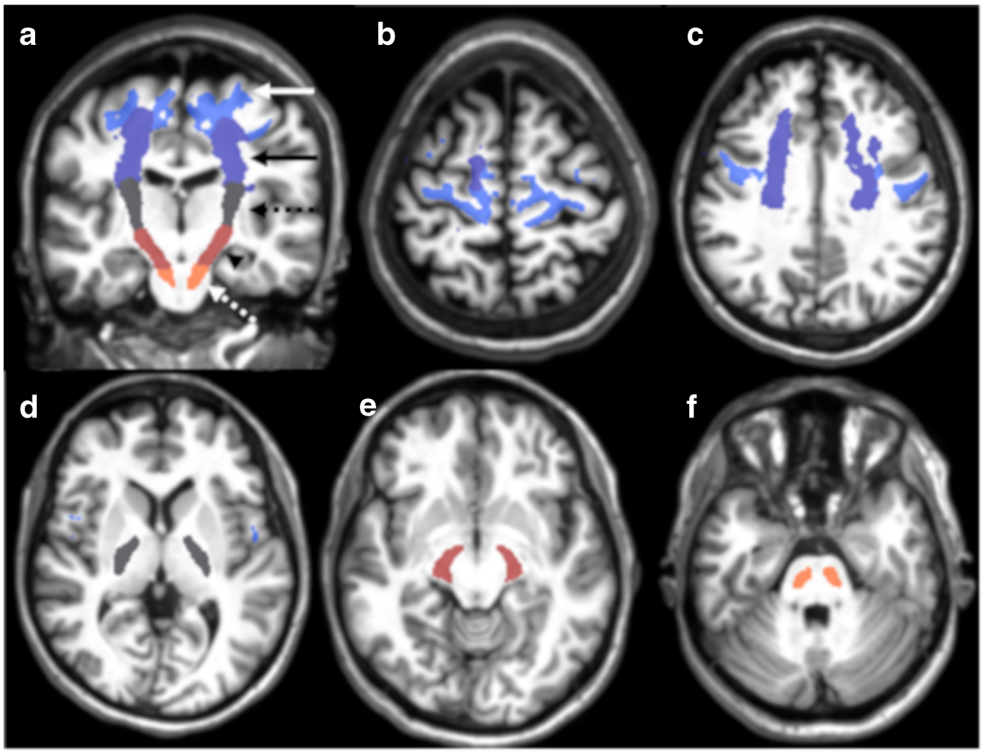

Fig. 1 CST segmented in 5 labels (**a**), precentral gyrus (white arrow) (**b**), superior corona radiata (black arrow) (**c**), posterior limb of internal capsule (black dotted arrow) (**d**), cerebral peduncle (black arrow head) (**e**), and basis pontis (white dotted arrow) (**f**)

Table 1 Cohort 1 mean FA, MD, RD, and AD values in SCA3 and control subjects

CST labels		DTI measures							
		FA	*p* value	MD (10^{-3})	*p* value	RD (10^{-3})	*p* value	AD (10^{-3})	*p* value
RPCG	SCA3	0.5721 ± 0.0369	*0.007*	0.4071 ± 0.0682	0.423	0.2710 ± 0.0618	0.184	0.6791 ± 0.0829	0.977
	Control	0.5929 ± 0.0160		0.3966 ± 0.0140		0.2552 ± 0.0132		0.6796 ± 0.0204	
LPCG	SCA3	0.5907 ± 0.0364	*0.009*	0.4064 ± 0.0690	0.349	0.2633 ± 0.0617	0.142	0.6926 ± 0.0854	0.889
	Control	0.6098 ± 0.0114		0.3941 ± 0.0122		0.2460 ± 0.0101		0.6903 ± 0.0207	
RSCR	SCA3	0.6931 ± 0.0487	0.145	0.3973 ± 0.0689	0.936	0.2142 ± 0.0659	0.507	0.7636 ± 0.0791	0.386
	Control	0.7068 ± 0.0114		0.3963 ± 0.0093		0.2059 ± 0.0083		0.7768 ± 0.0192	
LSCR	SCA3	0.7014 ± 0.0497	0.173	0.4013 ± 0.0720	0.929	0.2134 ± 0.0689	0.490	0.7768 ± 0.0830	0.350
	Control	0.7147 ± 0.0150		0.4001 ± 0.0105		0.2044 ± 0.0108		0.7920 ± 0.0243	
RPLIC	SCA3	0.7676 ± 0.0390	0.355	0.4238 ± 0.0629	0.853	0.1848 ± 0.0542	0.745	0.9019 ± 0.0867	1.000
	Control	0.7601 ± 0.0180		0.4261 ± 0.0186		0.1882 ± 0.0144		0.9019 ± 0.0404	
LPLIC	SCA3	0.7660 ± 0.0382	0.766	0.4335 ± 0.0656	0.652	0.1899 ± 0.0553	0.812	0.9209 ± 0.0928	0.528
	Control	0.7637 ± 0.0169		0.4393 ± 0.0214		0.1925 ± 0.0154		0.9331 ± 0.0454	
RCP	SCA3	0.7622 ± 0.0342	0.695	0.5384 ± 0.0669	0.215	0.2440 ± 0.0551	0.341	1.1274 ± 0.0983	0.175
	Control	0.7652 ± 0.0231		0.5214 ± 0.0294		0.2334 ± 0.0217		1.0971 ± 0.0668	
LCP	SCA3	0.7595 ± 0.0308	0.810	0.5646 ± 0.0708	0.154	0.2621 ± 0.0590	0.262	1.1699 ± 0.0991	0.106
	Control	0.7611 ± 0.0191		0.5443 ± 0.0275		0.2488 ± 0.0216		1.1349 ± 0.0570	
RBP	SCA3	0.6944 ± 0.0401	0.534	0.4244 ± 0.0719	0.502	0.2276 ± 0.0601	0.624	0.8182 ± 0.1054	0.417
	Control	0.6892 ± 0.0198		0.4148 ± 0.0262		0.2218 ± 0.0174		0.8003 ± 0.0533	
LBP	SCA3	0.6970 ± 0.0417	0.434	0.4261 ± 0.0681	0.399	0.2272 ± 0.0583	0.549	0.8240 ± 0.0952	0.306
	Control	0.6897 ± 0.0264		0.4137 ± 0.0377		0.2200 ± 0.0278		0.8015 ± 0.0680	

CST corticospinal tract, *SCA3* spinocerebellar ataxia type 3, *RPCG* right precentral gyrus, *LPCG* left precentral gyrus, *RSCR* right superior corona radiata, *LSCR* left superior corona radiata, *RPLIC* right posterior limb of internal capsule, *LPLIC* left posterior limb of internal capsule, *RCP* right cerebral peduncle, *LCP* left cerebral peduncle, *RBP* right basis pontis, *LBP* left basis pontis

Table 2 Cohort 2 mean FA, MD, RD, and AD values in SCA3 and control subjects

CST labels		DTI measures							
		FA	*p* value	MD (10^{-3})	*p* value	RD (10^{-3})	*p* value	AD (10^{-3})	*p* value
RPCG	SCA3	0.4123 ± 0.0145	*< 0.001*	0.7409 ± 0.0341	0.282	0.5714 ± 0.0314	0.036	1.0798 ± 0.0428	0.071
	Control	0.4233 ± 0.0146		0.7354 ± 0.0347		0.5615 ± 0.0318		1.0831 ± 0.0433	
LPCG	SCA3	0.4345 ± 0.0161	*< 0.001*	0.7251 ± 0.0293	*< 0.001*	0.5482 ± 0.0280	*< 0.001*	1.0791 ± 0.0364	0.609
	Control	0.4466 ± 0.0148		0.7105 ± 0.0232		0.5307 ± 0.0233		1.0703 ± 0.0288	
RSCR	SCA3	0.4782 ± 0.0268	*< 0.001*	0.6920 ± 0.0343	*< 0.001*	0.4997 ± 0.0358	*< 0.001*	1.0766 ± 0.0416	0.761
	Control	0.4977 ± 0.0249		0.6799 ± 0.0345		0.4806 ± 0.0339		1.0786 ± 0.0444	
LSCR	SCA3	0.4881 ± 0.0276	*< 0.001*	0.6852 ± 0.0315	*< 0.001*	0.4907 ± 0.0338	*< 0.001*	1.0741 ± 0.0384	0.179
	Control	0.5081 ± 0.0246		0.6670 ± 0.0249		0.4670 ± 0.0268		1.0669 ± 0.0338	
RPLIC	SCA3	0.6422 ± 0.0265	*< 0.001*	0.6499 ± 0.0364	*< 0.001*	0.3715 ± 0.0327	*< 0.001*	1.2067 ± 0.0612	0.241
	Control	0.6613 ± 0.0205		0.6326 ± 0.0335		0.3507 ± 0.0282		1.1963 ± 0.0569	
LPLIC	SCA3	0.6455 ± 0.0276	*< 0.001*	0.6786 ± 0.0357	*< 0.001*	0.3870 ± 0.0357	*< 0.001*	1.2618 ± 0.0533	*0.040*
	Control	0.6619 ± 0.0238		0.6599 ± 0.0327		0.3666 ± 0.0330		1.2464 ± 0.0468	
RCP	SCA3	0.6181 ± 0.0368	*< 0.001*	0.8594 ± 0.0563	*0.001*	0.5204 ± 0.0610	*< 0.001*	1.5375 ± 0.0689	*< 0.001*
	Control	0.6560 ± 0.0279		0.7893 ± 0.0508		0.4484 ± 0.0474		1.4713 ± 0.0790	
LCP	SCA3	0.6262 ± 0.0397	*< 0.001*	0.9213 ± 0.0655	*< 0.001*	0.5561 ± 0.0722	*< 0.001*	1.6517 ± 0.0748	*< 0.001*
	Control	0.6586 ± 0.0338		0.8468 ± 0.0496		0.4839 ± 0.0536		1.5728 ± 0.0717	
RBP	SCA3	0.4957 ± 0.0347	*< 0.001*	0.7813 ± 0.0539	*< 0.001*	0.5586 ± 0.0529	*< 0.001*	1.2267 ± 0.0691	*< 0.001*
	Control	0.5478 ± 0.0251		0.7147 ± 0.0335		0.4838 ± 0.0297		1.1765 ± 0.0601	
LBP	SCA3	0.5080 ± 0.0345	< 0.001	0.8064 ± 0.0607	*< 0.001*	0.5665 ± 0.0578	*< 0.001*	1.2861 ± 0.0808	*< 0.001*
	Control	0.5530 ± 0.0277		0.7366 ± 0.0326		0.4925 ± 0.0308		1.2248 ± 0.0589	

CST corticospinal tract, *SCA3* spinocerebellar ataxia type 3, *RPCG* right precentral gyrus, *LPCG* left precentral gyrus, *RSCR* right superior corona radiata, *LSCR* left superior corona radiata, *RPLIC* right posterior limb of internal capsule, *LPLIC* left posterior limb of internal capsule, *RCP* right cerebral peduncle, *LCP* left cerebral peduncle, *RBP* right basis pontis, *LBP* left basis pontis

obtained in DTI studies, and reflect the directionality and the average magnitude of water molecules motion, respectively. Axial diffusivity (AD) is the value of the primary eigenvector, which represents the diffusivity along the axon axis. Radial diffusivity (RD) is an average of diffusion direction perpendicular to the axon axis. We found no significant differences in CST diffusivity parameters of SCA3 patients scanned at 1.5 T (group 1), except for reduced FA at the PCG. In contrast, we found significant differences in almost all DTI measures (FA, MD, RD, and AD) along the CST of SCA3/MJD patients scanned at 3.0 T. Such discrepancy may be due to technical acquisition issues, such as the difference in magnetic field (1.5 T vs 3.0 T, respectively), methodology used to compute the diffusion parameters by the employed software, echo time (TE = 70 ms and 61 ms, respectively), gradient strength, and *b*-value (700 s/mm^2 vs 1000 s/mm^2, respectively) [21–23]. Another possible explanations are the sample size in each cohort (29 vs 91), which may have turned cohort 1 underpowered to detect subtle diffusivity changes, and the differences regarding the age difference of the SCA3 patients between cohort 1 and cohort 2 (40.5 ± 10.5 vs 48.16 ± 12.79) may have also interfered with the values of DTI parameters.

SCA3 is classically associated with neurodegeneration, and the presence of neuronal intra-nuclear ataxin-3 inclusion bodies is a pathologic hallmark of the disease [6, 24, 25]. Studies demonstrate the presence of ataxin-3 inclusion bodies in degenerated as well as in spared central nervous system regions, including the corticospinal tract [7, 10]. More recent pathological studies in SCA3 patients found degeneration in gray matter in the motor cerebellothalamocortical loop (cerebellar dentate and fastigial nuclei, cerebellar Purkinje cell layer, pontine and thalamic ventral lateral nuclei) and severe depletion of giant Betz pyramidal cells in the primary motor cortex of terminal SCA3 patients [7]. White matter lesion damage is less severe, and the corticospinal tract is often spared in SCA3 [4, 7].

The difference in FA, MD, and RD values between SCA3 and control subjects in cohort 2 is suggestive of dysfunction in pyramidal tract, which is often spared in pathologic studies. In a similar way, D'Abreu et al. showed in a study with MR spectroscopy deep cerebral white matter dysfunction not found in previous pathologic studies [26]. Our results are in line with clinical findings, since pyramidal signs are one of the most common clinical manifestations in SCA3 and can be found in 74–82% of the patients [27, 28]. It is worth to highlight a rare presentation of SCA3 in which patients present spastic paraparesis without cerebellar ataxia or signs of cerebellar atrophy in MRI studies [29, 30]. This rare presentation reinforces that degeneration of the pyramidal tract is a feature of SCA3. It would be interesting in future study to compare

Fig. 2 Relative difference of the mean FA, MD, RD, and AD (in percentage) between SCA3 and control subjects in cohort 2

the corticospinal tract with the brainstem and cerebellar white matter using DTI in SCA3 patients presenting with spastic paraparesis.

Some studies proposed a non-invasive method to differentiate axon and myelin pathology using DTI technique. Initial researches suggest that reduction in AD values is associated with axonal loss, like in transaxonal degeneration, and increase in RD values is associated with myelin loss [31–33]. The results obtained in cohort 2 showed increase in RD values in all the labels of pyramidal tract of the SCA3 patients compared with control subjects, suggesting that myelin loss is present in CST degeneration.

Different from RD, which showed widespread alteration, the AD values had significant between-group differences only in the lower segments of CST (CP and BP). This find may reinforce that the axonal damage is more severe (and may appears first) in the brainstem. It can also indicate that the myelin sheath microstructural damage precedes axonal degeneration.

In the comparison between the labels of CST, we notice that FA in BP had the greatest difference between SCA3 and control subjects, and the PCG white matter had the smallest difference between SCA3 and controls subjects, indicating more severe microstructural lesion in the lower segments of CST than in upper segments. This find may be an indicative of a retrograde degeneration (dying back degeneration) of the CST in SCA3 patients. In a research using DTI to quantify the CST, damage in patients with lateral amyotrophic sclerosis (ASL) showed greatest decrease in FA and ADC values in BP than in PLIC and corona radiata, suggesting a dying back neurodegeneration [34]. In the same year, Fisher et al. used a model with mutant mouse to suggest that ASL is distal axonopathy with a dying back degeneration mechanism. In this research, they found earliest degeneration in neuromuscular junction followed by motor axon from the ventral root and motor neuron in spinal cord [35].

The use of graduation scales for ataxia is well established in clinical practice and researches. The SARA is based on a semiquantitative assessment of the impairment related to the ataxia and is composed of eight items: gait, stance, sitting, speech disturbance, finger chase, nose-finger test, fast alternating hand movements, and heel-shin slide [16]. Oculomotor function and non-ataxia symptoms are not included in the evaluation. It has been validated in large cohorts of spinocerebellar ataxia patients, and did not show major ceiling of floor effect. It has the advantage of being a simple and fast scale to administer in clinical practice, with a high interrater reliability [16, 36–39].

A moderate correlation was found between FA, MD, and RD values of the CST with ataxia severity (SARA) in SCA3 subjects in cohort 2. Previous DTI and studies also found significant correlation between FA values in non-cerebellar regions (frontal, thalamic, and midbrain white matter) and SARA [40]. This suggests that non-cerebellar motor dysfunction may influence in ataxia severity in SCA3.

Our study has some limitations. Firstly, the patients were selected retrospectively and the image acquisition was obtained with different MRI parameters, as exposed before. Secondly, we analyzed the pyramidal tract in superior corona radiate, posterior limb of internal capsule, and cerebral peduncle, and the pyramidal tract is not the only white matter tract in those structures.

In conclusion, this study demonstrated CST tracts dysfunction in patients with SCA3 using DTI technique in 3.0 T scanner and a moderate correlation of FA, MD, and RD with ataxia severity (SARA). Moreover, we showed greatest microstructural damage in lower segments of CST, indicating the possibility of a dying back neurodegeneration of this tract. Finally, the different results obtained in 1.5 T and 3.0 T scanners showed the importance of improving DTI protocol in future clinical trials.

Funding No funding was received for this study.

Compliance with ethical standards

Conflict of interest The authors declare that they have no conflict of interest.

Ethical approval All procedures performed in the studies involving human participants were in accordance with the ethical standards of the institutional and/or national research committee and with the 1964 Helsinki Declaration and its later amendments or comparable ethical standards.

Informed consent Informed consent was obtained from all individual participants included in the study.

References

1. Kawaguchi Y, Okamoto T, Taniwaki M, Aizawa M, Inoue M, Katayama S, Kawakami H, Nakamura S, Nishimura M, Akiguchi I, Kimura J, Narumiya S, Kakizuka A (1994) CAG expansions in a novel gene for Machado-Joseph disease at chromosome 14q32.1. Nat Genet 8:221–228. https://doi.org/10.1038/ng1194-221
2. Nakano K, Spence A, Dawson D (1972) Machado disease. Neurology 22:49–55. https://doi.org/10.1212/WNL.22.1.49
3. Rosenberg RN, Fowler HL, de Magalhães J et al (1977) Azorean disease of the nervous system. N Engl J Med 297:729–730. https://doi.org/10.1056/NEJM197709292971318
4. Dürr A, Stevanin G, Cancel G et al (1996) Spinocerebellar ataxia 3 and Machado-Joseph disease: clinical, molecular, and neuropathological features. Ann Neurol 39:490–499. https://doi.org/10.1002/ana.410390411
5. Pedroso JL, França MC, Braga-Neto P et al (2013) Nonmotor and extracerebellar features in Machado-Joseph disease: a review. Mov Disord 28:1200–1208. https://doi.org/10.1002/mds.25513
6. Riess O, Rüb U, Pastore A, Bauer P, Schöls L (2008) SCA3: neurological features, pathogenesis and animal models. Cerebellum 7:125–137. https://doi.org/10.1007/s12311-008-0013-4
7. Rüb U, Brunt ER, Deller T (2008) New insights into the pathoanatomy of spinocerebellar ataxia type 3 (Machado-Joseph disease). Curr Opin Neurol 21:111–116. https://doi.org/10.1097/WCO.0b013e3282f7673d
8. de Rezende TJR, D'Abreu A, Guimarães RP et al (2015) Cerebral cortex involvement in Machado-Joseph disease. Eur J Neurol 22:277–283. https://doi.org/10.1111/ene.12559
9. Murata Y, Yamaguchi S, Kawakami H, Imon Y, Maruyama H, Sakai T, Kazuta T, Ohtake T, Nishimura M, Saida T, Chiba S, Oh-i T, Nakamura S (1998) Characteristic magnetic resonance imaging findings in Machado-Joseph disease. Arch Neurol 55:33–37. https://doi.org/10.1001/archneur.55.1.33
10. Onodera O, Idezuka J, Igarashi S, Takiyama Y, Endo K, Takano H, Oyake M, Tanaka H, Inuzuka T, Hayashi T, Yuasa T, Ito J, Miyatake T, Tsuji S (1998) Progressive atrophy of cerebellum and brainstem as a function of age and the size of the expanded CAG repeats in the MJD1 gene in Machado-Joseph disease. Ann Neurol 43:288–296. https://doi.org/10.1002/ana.410430305
11. Peng H, Liang X, Long Z, Chen Z, Shi Y, Xia K, Meng L, Tang B, Qiu R, Jiang H (2019) Gene-related cerebellar neurodegeneration in SCA3/MJD: a case-controlled imaging-genetic study. Front Neurol 10:1–10. https://doi.org/10.3389/fneur.2019.01025
12. Farrar MA, Vucic S, Nicholson G, Kiernan MC (2016) Motor cortical dysfunction develops in spinocerebellar ataxia type 3. Clin Neurophysiol 127:3418–3424. https://doi.org/10.1016/j.clinph.2016.09.005
13. Jhunjhunwala K, Prashanth DK, Netravathi M, Jain S, Purushottam M, Pal PK (2013) Alterations in cortical excitability and central motor conduction time in spinocerebellar ataxias 1, 2 and 3: a comparative study. Parkinsonism Relat Disord 19:306–311. https://doi.org/10.1016/j.parkreldis.2012.11.002
14. Wu X, Liao X, Zhan Y, Cheng C, Shen W, Huang M, Zhou Z, Wang Z, Qiu Z, Xing W, Liao W, Tang B, Shen L (2017) Microstructural alterations in asymptomatic and symptomatic patients with spinocerebellar ataxia type 3: a tract-based spatial statistics study. Front Neurol 8:1–9. https://doi.org/10.3389/fneur.2017.00714
15. Rezende TJR, de Paiva JLR, Martinez ARM, Lopes-Cendes I, Pedroso JL, Barsottini OGP, Cendes F, França MC Jr (2018) Structural signature of SCA3: from presymptomatic to late disease stages. Ann Neurol 84:401–408. https://doi.org/10.1002/ana.25297
16. Schmitz-Hübsch T, du Montcel ST, Baliko L, Berciano J, Boesch S, Depondt C, Giunti P, Globas C, Infante J, Kang JS, Kremer B, Mariotti C, Melegh B, Pandolfo M, Rakowicz M, Ribai P, Rola R, Schöls L, Szymanski S, van de Warrenburg B, Dürr A, Klockgether T, Fancellu R (2006) Scale for the assessment and rating of ataxia: development of a new clinical scale. Neurology 66:1717–1720. https://doi.org/10.1212/01.wnl.0000219042.60538.92
17. Zhuang J, Hrabe J, Kangarlu A, Xu D, Bansal R, Branch CA, Peterson BS (2006) Correction of eddy-current distortions in diffusion tensor images using the known directions and strengths of diffusion gradients. J Magn Reson Imaging 24:1188–1193. https://doi.org/10.1002/jmri.20727
18. Woods RP, Grafton ST, Holmes CJ, Cherry SR, Mazziotta JC (1998) Automated image registration: I. General methods and intrasubject, intramodality validation. J Comput Assist Tomogr 22:139–152. https://doi.org/10.1097/00004728-199801000-00027
19. Tang X, Yoshida S, Hsu J, Huisman TAGM, Faria AV, Oishi K, Kutten K, Poretti A, Li Y, Miller MI, Mori S (2014) Multi-contrast multi-atlas parcellation of diffusion tensor imaging of the human brain. PLoS One 9:e96985. https://doi.org/10.1371/journal.pone.0096985
20. Towns J, Cockerill T, Dahan M, Foster I, Gaither K, Grimshaw A, Hazlewood V, Lathrop S, Lifka D, Peterson GD, Roskies R, Scott JR, Wilkins-Diehr N (2014) XSEDE: Accelerating scientific discovery. Comput Sci Eng 16:62–74. https://doi.org/10.1109/MCSE.2014.80

21. Qin W, Yu CS, Zhang F et al (2009) Effects of echo time on diffusion quantification of brain white matter at 1.5 T and 3.0 T. Magn Reson Med 61:755–760. https://doi.org/10.1002/mrm.21920
22. Chou MC, Kao EF, Mori S (2013) Effects of b-value and echo time on magnetic resonance diffusion tensor imaging-derived parameters at 1.5 t: a voxel-wise study. J Med Biol Eng 33:45–50. https://doi.org/10.5405/jmbe.1126
23. Chung AW, Thomas DL, Ordidge RJ, Clark CA (2013) Diffusion tensor parameters and principal eigenvector coherence: Relation to b-value intervals and field strength. Magn Reson Imaging 31:742–747. https://doi.org/10.1016/j.mri.2012.11.014
24. Paulson HL, Das SS, Crino PB, Perez MK, Patel SC, Gotsdiner D, Fischbeck KH, Pittman RN (1997) Machado-Joseph disease gene product is a cytoplasmic protein widely expressed in brain. Ann Neurol 41:453–462. https://doi.org/10.1002/ana.410410408
25. Wu Y, Peng Y, Wang Y (2014) An insight into advances in the pathogenesis and therapeutic strategies of spinocerebellar ataxia type 3. Rev Neurosci 26:95–104. https://doi.org/10.1515/revneuro-2014-0040
26. D'Abreu A, França M, Appenzeller S et al (2009) Axonal dysfunction in the deep white matter in Machado-Joseph disease. J Neuroimaging 19:9–12. https://doi.org/10.1111/j.1552-6569.2008.00260.x
27. Jardim LB, Pereira ML, Silveira I, Ferro A, Sequeiros J, Giugliani R (2001) Neurologic findings in Machado-Joseph disease. Arch Neurol 58:899. https://doi.org/10.1001/archneur.58.6.899
28. Pulido-Valdeolivas I, Gómez-Andrés D, Sanz-Gallego I, Rausell E, Arpa J (2016) Patterns of motor signs in spinocerebellar ataxia type 3 at the start of follow-up in a reference unit. Cerebellum Ataxias 3:1–10. https://doi.org/10.1186/s40673-016-0042-6
29. Guang WY, Du J, Ling WJ et al (2009) Six cases of SCA3/MJD patients that mimic hereditary spastic paraplegia in clinic. J Neurol Sci 285:121–124. https://doi.org/10.1016/j.jns.2009.06.027
30. Song Y, Liu Y, Zhang N, Long L (2015) Spinocerebellar ataxia type 3/machado-joseph disease manifested as spastic paraplegia: a clinical and genetic study. Exp Ther Med 9:417–420. https://doi.org/10.3892/etm.2014.2136
31. Song SK, Yoshino J, Le TQ et al (2005) Demyelination increases radial diffusivity in corpus callosum of mouse brain. Neuroimage 26:132–140. https://doi.org/10.1016/j.neuroimage.2005.01.028
32. Song SK, Sun SW, Ju WK, Lin SJ, Cross AH, Neufeld AH (2003) Diffusion tensor imaging detects and differentiates axon and myelin degeneration in mouse optic nerve after retinal ischemia. Neuroimage 20:1714–1722. https://doi.org/10.1016/j.neuroimage.2003.07.005
33. Sun SW, Liang HF, Trinkaus K, Cross AH, Armstrong RC, Song SK (2006) Noninvasive detection of cuprizone induced axonal damage and demyelination in the mouse corpus callosum. Magn Reson Med 55:302–308. https://doi.org/10.1002/mrm.20774
34. Karlsborg M, Rosenbaum S, Wiegell MR, Simonsen H, Larsson HBW, Werdelin LM, Gredal O (2004) Corticospinal tract degeneration and possible pathogenesis in ALS evaluated by MR diffusion tensor imaging. Amyotroph Lateral Scler Other Mot Neuron Disord 5:136–140. https://doi.org/10.1080/14660820410018982
35. Fischer LR, Culver DG, Tennant P, Davis AA, Wang M, Castellano-Sanchez A, Khan J, Polak MA, Glass JD (2004) Amyotrophic lateral sclerosis is a distal axonopathy: evidence in mice and man. Exp Neurol 185:232–240. https://doi.org/10.1016/j.expneurol.2003.10.004
36. Yabe I, Matsushima M, Soma H, Basri R, Sasaki H (2008) Usefulness of the scale for assessment and rating of ataxia (SARA). J Neurol Sci 266:164–166. https://doi.org/10.1016/j.jns.2007.09.021
37. Bürk K, Sival DA (2018) Scales for the clinical evaluation of cerebellar disorders. Handb Clin Neurol 154:329–339. https://doi.org/10.1016/B978-0-444-63956-1.00020-5
38. Schmitz-Hübsch T, Fimmers R, Rakowicz M et al (2010) Responsiveness of different rating instruments in spinocerebellar ataxia patients. Neurology 74:678–684. https://doi.org/10.1212/WNL.0b013e3181d1a6c9
39. Paap BK, Roeske S, Durr A, Schöls L, Ashizawa T, Boesch S, Bunn LM, Delatycki MB, Giunti P, Lehéricy S, Mariotti C, Melegh J, Pandolfo M, Tallaksen CME, Timmann D, Tsuji S, Schulz JB, van de Warrenburg BP, Klockgether T (2016) Standardized assessment of hereditary ataxia patients in clinical studies. Mov Disord Clin Pract 3:230–240. https://doi.org/10.1002/mdc3.12315
40. Kang JS, Klein JC, Baudrexel S, Deichmann R, Nolte D, Hilker R (2014) White matter damage is related to ataxia severity in SCA3. J Neurol 261:291–299. https://doi.org/10.1007/s00415-013-7186-6